

Pd/SiO<sub>2</sub>I. *In Situ* X-Ray Diffraction Studies during Treatment and HydrogenolysisR. K. NANDI, R. PITCHAI, S. S. WONG,<sup>1</sup> J. B. COHEN, R. L. BURWELL, JR., AND J. B. BUTT*Ipatieff Catalytic Laboratory and Department of Materials Science and Engineering, Northwestern University, Evanston, Illinois 60201*

Received November 6, 1980; revised February 19, 1981

Simple techniques for studies of X-ray diffraction from Pd/SiO<sub>2</sub> catalysts during catalytic reactions are reported here. The catalytic activity of Pd/SiO<sub>2</sub> of low percentage metal exposed for methylcyclopropane hydrogenolysis at 0°C is less for catalyst cooled from 450°C in H<sub>2</sub> than for that cooled in He. This effect appears to result from differing amounts of hydride formation. Ease of formation of hydride decreases with decreasing Pd particle size. Exposing the catalysts with  $D_n = 13.8$  and 29.3% to hydrogen at ~25°C results in nearly complete conversion of particles of Pd to hydride. Purging with helium (even at 0°C) reconverts the hydride to palladium, but this reconversion exhibits an induction period; hydride formation is more rapid. Passing hydrogen plus methylcyclopropane results in the conversion into hydride of a substantial fraction of catalyst particles originally present as palladium. The palladium hydride particles of catalyst produced by cooling from 450°C in H<sub>2</sub> remain as PdH<sub>0.7</sub> during the hydrogenolysis reaction. The lattice parameter of palladium particles is indistinguishable from that of bulk palladium, at least for particle diameters  $\geq 45$  Å.

## INTRODUCTION

It is well known that palladium absorbs hydrogen [the discovery was made in 1866 by Thomas Graham (1)] and at a sufficient concentration of H<sub>2</sub>, transforms to the  $\beta$ -hydride phase. Since palladium is used extensively in catalytic reactions involving hydrogen, it is imperative to know whether it has been converted (partially or fully) to the hydride phase under reaction conditions. In many reactions, an observed decrease in activity could be due to hydride formation; this area has been reviewed by Palczewska (2). A recent report (3) indicates that all particles of the Pd black studied (diameters of 70–1400 Å) were converted to hydride by exposure to hydrogen at 30 and 60°C. Only one previous research report (4) has directly examined by X-ray diffraction the amount of palladium hydride

present during a catalytic reaction (the hydrogenation of acetylene on a Pd/Al<sub>2</sub>O<sub>3</sub> catalyst). However, the authors do not present the diffraction profiles recorded during the reaction nor do they describe how they could separate or identify the broad peaks of Pd and  $\beta$ -Pd-H from the strong peaks of the  $\gamma$ -Al<sub>2</sub>O<sub>3</sub> support, especially with the limited amount of catalyst material they employed (spread as a thin film of powder on a glass plate). To illustrate the difficulties, Fig. 1 shows the diffraction pattern of a Pt/Al<sub>2</sub>O<sub>3</sub> catalyst (26% metal percentage exposed, 0.8 wt% Pt) obtained with Ni-filtered CuK $\alpha$  radiation from a conventional X-ray source operated at 50 kV and 11 mA. The catalyst (3.5 g) was in a cell with a mica window and was ~7 mm thick. The strong Al<sub>2</sub>O<sub>3</sub> peaks obliterate any peaks resulting from Pt. As the positions of the peaks of Pd and Pd-H (indicated in the figure) are close to but lower in intensity than those for Pt, it is unclear to us how the authors could have

<sup>1</sup> Present address: Mobil Research and Development Corporation, Princeton, N.J. 08540.

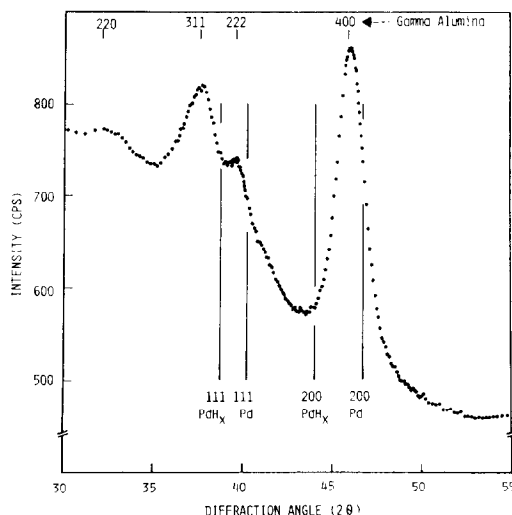


FIG. 1. Diffraction pattern, Pt/ $\gamma$ -Al<sub>2</sub>O<sub>3</sub>,  $D_h = 26\%$ , 0.8 wt% Pt. Pd and Pt peaks are very similar in  $2\theta$  positions (differing by  $\sim 0.3^\circ 2\theta$  for the 111 peak) so that the pattern for Pd on  $\gamma$ -Al<sub>2</sub>O<sub>3</sub> would be quite similar. There are no Pt peaks detectable and the indicated locations of the Pd and PdH<sub>x</sub> peaks illustrate the difficulty in detecting these phases in the presence of Al<sub>2</sub>O<sub>3</sub> support.

recorded peaks from both phases in any quantitative fashion.

Boudart and Hwang (5) found that the solubility of hydrogen in Pd at a given temperature and pressure decreased with decreasing particle size, perhaps because the pressure required for hydride formation increases with decreasing size. Aben (6) has shown the total hydrogen uptake in the  $\beta$ -hydride phase to decrease with decreasing particle size. It is clearly important to confirm that hydride actually forms during reactions and to explore the conditions for its formation and disappearance.

As a continuation of our studies on the properties of supported metal catalysts (7–14), we have prepared a series of Pd/silica gel catalysts with varying percentage metal exposed. For these Pd catalysts, the formation and removal of the  $\beta$ -hydride phase both during catalytic reactions and after specific pretreatments can be identified by X-ray diffraction since the amorphous support does not interfere appreciably with the diffraction peaks of either Pd or  $\beta$ -Pd–H. In

this paper, we report on techniques for quantitative *in situ* studies of the diffraction pattern of catalysts, and the results of studies of Pd/SiO<sub>2</sub> catalysts during exposure to various gas environments, including hydrogen plus methylcyclopropane.

## EXPERIMENTAL

### Catalyst Preparation and Characterization

A series of catalysts of different percentage metal exposed (metal loading  $\sim 2$  wt% or less) was prepared by Dr. N. Takahashi in our laboratory by ion exchange of Pd(NH<sub>3</sub>)<sub>4</sub>(NO<sub>3</sub>)<sub>2</sub> with Davison grade-62 silica gel (80–100 mesh) at a constant pH of 9.5, followed by drying and reduction. The percentage metal exposed was determined by chemisorption using H<sub>2</sub> pulse technique (7). The details of the preparation and characterization by chemisorption can be found in Ref. (15).

### Reaction

Hydrogenolysis of methylcyclopropane was carried out over the different catalysts in a differential reactor. The reaction mixture was prepared by flowing hydrogen through a saturator containing methylcyclopropane at  $-52^\circ\text{C}$ . This gave H<sub>2</sub>:C<sub>4</sub>H<sub>8</sub> = 16:1. This mixture passed through a trap of MnO/SiO<sub>2</sub> just before entering the reactor. The trap is reported to reduce the proportion of O<sub>2</sub> to less than 0.001 ppm (16). Other experimental details have been described in Ref. (9).

### X-Ray Measurements

The X-ray diffraction patterns of the catalysts were examined first in the as-prepared state. The experimental technique and the analysis procedure (including Fourier analysis of peak shape) are the same as those described in Ref. (8).

The *in situ* X-ray characterization of these catalysts was performed in both batch and flow experiments. In the batch process, the stored catalyst was placed in a specially

constructed specimen holder (cell) transparent to X rays which could be attached to a gas train. Various pretreatments were performed on the same batch of the catalyst sequentially without exposure to air. The details of the construction of the cell and the gas treatment apparatus have been given in Ref. (12). Some 3.5 g of catalysts was employed. After each pretreatment, the catalyst was cooled to room temperature and kept in the desired gaseous environment by closing the valves attached to the cell. The cell was then transferred from the gas train to the diffractometer for recording the diffraction pattern. Ni-filtered  $\text{CuK}\alpha$  radiation from conventional X-ray generators (operated at 50 kV and 11 mA) coupled with a diffractometer controlled by a 16K PDP8E minicomputer was employed for recording the pattern.

The various treatments are outlined in Table 1.

In the flow experiments, the X-ray measurements were obtained during the hydrogenolysis of methylcyclopropane. A special cell (Fig. 2), different from the one used for the batch process, was constructed from Pyrex glass. This cell had two portions: (a) a tubular section and (b) a reaction section.

TABLE 1  
Pretreatments

Treatment	Condition
a (Standard)	$\text{O}_2$ , 300°C, 0.5 hr $\text{H}_2$ , 300°C, 1 hr $\text{He}$ , 450°C, 1 hr Cool to 25°C in $\text{He}$
b	$\text{O}_2$ , 300°C, 0.5 hr $\text{H}_2$ , 25°C, 1 hr
c	$\text{O}_2$ , 300°C, 0.5 hr $\text{H}_2$ , 450°C, 1 hr Cool to 25°C in $\text{H}_2$
d	$\text{O}_2$ , 300°C, 0.5 hr $\text{H}_2$ , 450°C, 1 hr Cool to 25°C in $\text{He}$

Note. A brief purge of  $\text{He}$  was employed between flows of  $\text{O}_2$  and  $\text{H}_2$ .

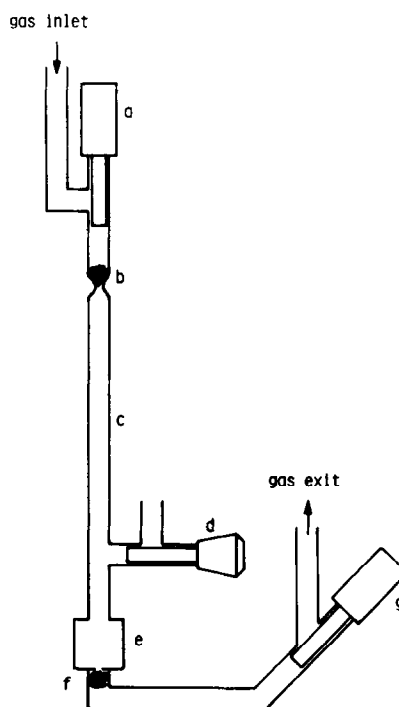


FIG. 2. Cell for diffraction studies during hydrogenolysis: a, g—Teflon needle valve; b, f—glass wool; c—pretreatment section; d—rotflow valve for inserting catalyst in the cell; e—reaction region.

The tubular section was made of  $\frac{1}{8}$ -in. Pyrex tubing. The glass back of the reaction section was cylindrical in shape, whereas the front had a very thin ( $\sim 0.01$  mm thick) scratch-free flat mica window attached with "Torr Seal." The window was about  $1 \times 1$  cm. The catalysts were pretreated in the tubular section as a fluidized bed. Then, with gas flowing, the catalyst was transferred to the reaction section by tilting the cell. The cell was then mounted on a diffractometer for *in situ* studies. The cell was preceded by two helices of  $\frac{1}{8}$ -in. copper tubing cooled in ice. A flow of nitrogen cooled by liquid nitrogen was directed onto the cell. During hydrogenolysis, the temperature of the gas surrounding the cell was  $-10^\circ\text{C}$ . About 0.3 g of catalyst was employed and the gas flow rate was 180  $\text{cm}^3/\text{min}$ . The product was sampled and analyzed by gas chromatography at different times during a run to determine the

extent of hydrogenolysis (9). Conversions were 20% or less. At this conversion, the adiabatic temperature rise would have been about 50°C. The actual temperature profile through the bed of catalyst in the cell was unknown. For these flow experiments we used Zr-filtered MoK $\alpha$  radiation from a 12-kW Rigaku rotating-anode X-ray generator. The peaks with this radiation are narrower than CuK $\alpha$  peaks, since line broadening due to particle size is proportional to the wavelength, and intensities from our rotating anode are about ten times higher than those from a sealed X-ray tube. Furthermore, the mica window absorbed only ~20–30% of the MoK $\alpha$  compared to ~60–70% of the CuK $\alpha$ . These procedures permitted the study of the time-dependent structure of the Pd/SiO<sub>2</sub> catalysts during reaction. Two kinds of measurements were made. In point counting,  $2\theta$  was kept fixed at the 111 diffraction peak of either Pd or PdH<sub>x</sub> and total counts were recorded over a 10-sec interval. In the other, the region including the 111 peaks of both Pd and PdH<sub>x</sub> (~1–2°  $2\theta$ ) was scanned stepwise with steps of 0.1°  $2\theta$ . The count time for each step was 10 sec. The total time required for a scan was ~200 sec. Typical

intensities for such a measurement are shown in Figs. 6–8.

#### RESULTS AND DISCUSSION

X-Ray measurements have been made primarily on two Pd/SiO<sub>2</sub> catalysts having percentages exposed ( $D_h$ ) of 13.8 and 29.3 ( $D_h$  symbolizes percentage exposed measured by the H<sub>2</sub> pulse chemisorption technique). Peaks from catalysts with higher  $D_h$  (approx  $\geq 50\%$ ) could not be detected because of low metal loading and the smaller crystallite sizes. The crystallite sizes in the  $\langle 111 \rangle$ ,  $\langle 100 \rangle$ , and  $\langle 110 \rangle$  directions, the microstrain along the  $\langle 111 \rangle$  direction, the percentage metal exposed, metal weight fraction and the lattice parameter are given in Table 2 for the two catalysts stored in air after their preparation. Since the 400 reflection is very weak in intensity and the higher order of the 220 reflection could not be detected, we report only the crystallite sizes in the directions  $\langle 100 \rangle$  and  $\langle 110 \rangle$ , assuming that the microstrain is an average of constant strain and constant stress conditions which is the usual distribution observed in cold-worked metals (17). The sizes are almost the same in different crystallographic directions, so that

TABLE 2  
X-Ray Characterization of Stored Pd/SiO<sub>2</sub> Catalysts

Catalyst, $D_h$ (%)	Crystallite sizes ( $D$ ) (in Å) along the directions by Fourier analysis			$\langle \epsilon_{L=50 \text{ Å}}^2 \rangle_{111}^{1/2 a}$ (10 <sup>-3</sup> )	$D_x^b$ (%)	$D_h^c$ (%)	Pd wt% <sup>d</sup> from (estimated error: 10%)		Loading during preparation (wt%)	Lattice parameter <sup>e</sup> (Å)
	$\langle 111 \rangle$	$\langle 100 \rangle$	$\langle 110 \rangle$				111 peak	200 peak		
13.8	93	88	104	3.1	11.7	13.8	3.4	2.8	2.09	3.8887 (30)
29.3	51	45	39	2.9	24.7	29.3	2.2	2.0	2.09	3.8924 (40)

<sup>a</sup> Microstrain along  $\langle 111 \rangle$  direction at a column length  $L = 50 \text{ Å}$ .

<sup>b</sup> Percentage metal exposed calculated from average particle size (see Ref. (8)).

<sup>c</sup> Percentage metal exposed determined from chemisorption.

<sup>d</sup> Metal loading has been calculated by comparing the integrated intensities of 111 and 200 peaks of the catalysts with that from a standard, prepared by mixing ~2 wt% Pd black with silica gel (error associated with this calculation is ~10%; Uncertainty is based on location of background line).

<sup>e</sup> Lattice parameter values are calculated by considering 111, 200, 220, 311, 222, and 400 peaks. The value for bulk Pd (Ref. (17)) is 3.8907 Å. Values in parentheses are the standard deviation.

the particles are nearly equiaxed in shape as was the case for Pt/SiO<sub>2</sub> of similar  $D_h$  (8). The microstrain ( $\langle \epsilon_{L=50 \text{ Å}}^2 \rangle^{1/2} \sim 3 \times 10^{-3}$  along the  $\langle 111 \rangle$  direction) indicates a dislocation density of  $\sim 4 \times 10^{11}$  dislocations per square centimeter (see Ref. (8) for the equation linking these two quantities). The percentage metal exposed calculated from the average particle sizes agrees with that from chemisorption, which indicates that the crystallite size is the full Pd particle (as was the case for Pt (8)). The lattice parameter is close to the value for bulk metal (18). The metal weight fractions have been calculated by comparing the integrated intensities of both the 111 and 200 reflections of the catalysts with those from a standard prepared by mixing known amounts of Pd black with silica gel. The background for the peaks was selected by matching the pattern with that from pure silica gel.

The results of treatments with the batch process are given in Table 3. After the standard pretreatment (see Table 1) both catalysts show only peaks corresponding to

palladium (111, 200, 311, 222, and 400 reflections were also found). With CuK $\alpha$  radiation, the palladium 111 and 200 peaks appear near 40.1 and 46.6° 2 $\theta$ , respectively. However, the diffraction pattern of both the catalysts after treatments b and c shows strong peaks around 38.8 and 45° 2 $\theta$  accompanied by quite small peaks near those expected for pure palladium. The lattice parameter ( $\sim 4.04 \text{ Å}$ ) calculated from these shifted peaks corresponds to that of  $\beta$ -palladium hydride ( $\sim \text{PdH}_{0.7}$ , Ref. (19)). (111, 200, 311, 222 and 400 peaks from the hydride were detected.) By comparing the areas under the 111 reflection of  $\beta$ -palladium hydride and palladium, it has been estimated that after treatments b and c, about 90 and 80 vol% of the palladium has been converted to hydride for the 13.8 and 29.3% metal exposed catalysts, respectively. After pretreatment d, no hydride formation was detected. The crystallite sizes shown in Table 3 after pretreatments b and c are calculated from the 111 peak of  $\beta$ -palladium hydride assuming no strain. It

TABLE 3  
Effect of Different Pretreatments on Pd/SiO<sub>2</sub> Catalysts

Catalyst, $D_h$ (%)	Treatment	Crystallite sizes ( $D$ ) (in Å) along the direction		$\langle \epsilon_{L=50 \text{ Å}}^2 \rangle_{111}^{1/2}$ ( $10^{-3}$ )	Pd wt% from (error: 10%)		Loading during preparation (wt%)	Lattice parameter <sup>a</sup> (Å)
					111 peak	200 peak		
		$\langle 111 \rangle$	$\langle 100 \rangle$					
13.8	a	78	65	2.6	2.6	1.9	2.09	3.8917 (20)
	b <sup>b</sup>	74 <sup>c</sup>	—	—	—	—		4.0433 (20)
	c <sup>b</sup>	78 <sup>c</sup>	—	—	—	—		4.0391 (30)
	d	100	101	2.4	2.5	2.4		3.8927 (20)
29.3	a	52	35	2.4	2.0	1.9	2.09	3.8903 (60)
	b <sup>b</sup>	47 <sup>c</sup>	—	—	—	—		4.0418 (40)
	c <sup>b</sup>	44 <sup>c</sup>	—	—	—	—		4.0386 (30)
	d	56	46	2.4	1.9	1.9		3.8898 (60)

<sup>a</sup> Lattice parameter values are calculated considering 111, 200, 311, 222, and 400 peaks. Values in parentheses are the standard deviation.

<sup>b</sup> Treatments b and c form hydrides.

<sup>c</sup> Particle size values are determined from the 111 peak of  $\beta$ -palladium hydride assuming no strain.

is clear that the hydride forms throughout the Pd particles, not just at the surface, as the size is the same as that for the original Pd metal particles.

The palladium particle size distribution in the  $\langle 111 \rangle$  direction for the catalyst of  $D_h = 29.3\%$  is shown in Fig. 3. Included is the distribution for the catalyst after storage in air, after treatment a, after treatment c followed by a purge of He at 25°C for 15 min and after treatment d. The distributions show a tailing to larger sizes, with little effect of the treatment. This suggests that the distribution is due to atomic migration (20) or particle coalescence (21). The microstrain decreases appreciably with treatment. Note also that the lattice parameters are the same as those for the bulk metal, in agreement with Ref. (3). It is also worth noting that after treatments a and d, the metal loading calculated from the 111 peak alone for  $D_h = 13.8\%$  is in better agreement with the known loading than with the stored catalyst. This is perhaps due to some change in morphology during the treatment from a platelike form to a more nearly equiaxed shape. There was apparently no such change for  $D_h = 29.3\%$  as the value agrees with that from the original preparation.

During the studies of the catalytic activity of the Pd/SiO<sub>2</sub> catalysts for the hydro-

genolysis of methylcyclopropane, it was observed that the activities of the catalysts after the standard pretreatment (a in Table 1) were higher than after treatments c and d. This was also reported to be the case in the hydrogenation of acetylene (4). Typical plots of the turnover frequencies for isobutane formation after pretreatments c and d for the Pd/SiO<sub>2</sub> catalysts of varying dispersion are shown in Fig. 4 (from Ref. (22)). It is seen that the two catalysts of lowest  $D_h$  exhibited higher activity after cooling in helium than after cooling in hydrogen, while higher  $D_h$  samples had similar activity. A possible interpretation of this behavior is that formation of an inactive or less active hydride phase occurs in the catalysts with the larger Pd crystallites when they are cooled in hydrogen. The results of Boudart and Hwang (5) suggest that such a phase would not be found for the smaller crystallite catalyst.

To investigate the catalysts during these pretreatments, *in situ* X-ray studies were carried out. The sequence for these measurements is given in Fig. 5 and the diffraction peaks at various stages are presented in Figs. 6–8 for the catalyst with  $D_h = 13.8\%$ . The stored catalyst was first scanned to locate the  $2\theta$  position of maximum intensity for the Pd 111 peak. By remaining at that  $2\theta$  position and point counting every 10 sec, any phase transformation of palladium into palladium hydride

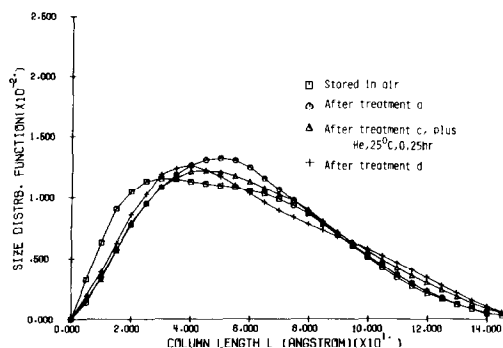


FIG. 3. Particle size distribution: probability of a given size vs distance,  $L$ , normal to the diffracting planes. From Fourier analysis of shape of 111 diffraction peak (see Ref. (8) for procedures) of  $D_h = 29.3\%$  Pd/SiO<sub>2</sub>.

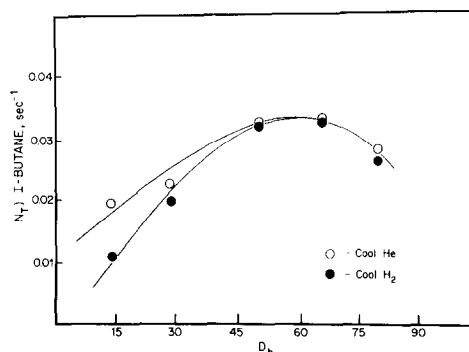


FIG. 4. Turnover frequency  $N_T$  for i-butane formation vs  $D_h$  determined by hydrogen chemisorption, after O<sub>2</sub>, 300°C, 0.5 hr; H<sub>2</sub>, 450°C, 1 hr.

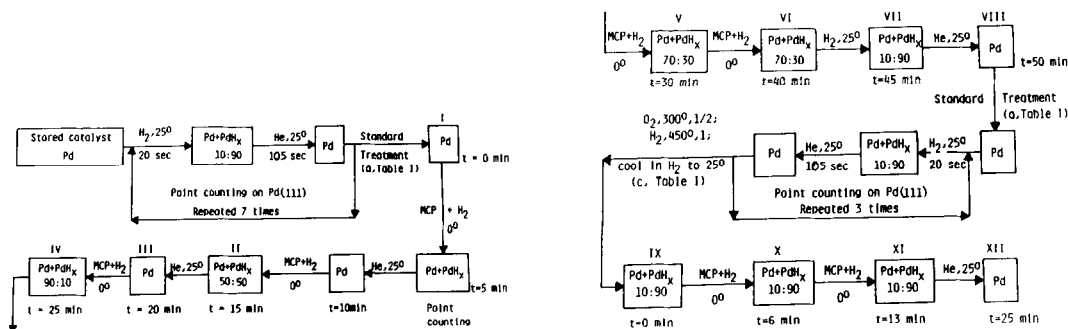


FIG. 5. Flow chart for studies of the effects of different treatments and of methylcyclopropane hydrogenolysis upon the diffraction pattern of  $D_h = 13.8\%$  Pd/SiO<sub>2</sub>. Rectangular boxes indicate that the sample was examined by X-ray diffraction. The step scanning procedure was employed except where point counting is indicated. Roman numerals represent the X-ray scans shown in Figs. 6–8;  $t$  is the time in minutes at which the scans were made. The ratios below the boxes represent the proportions of Pd and PdH<sub>x</sub> formed.

can be detected by the change in intensity. Hydrogen was then passed over the catalyst and the point counting continued. It is seen in Fig. 9a that the intensity was re-

duced almost to that of the background within 20 sec of starting the hydrogen flow. The flow was then switched to helium at the same flow rate. As shown in Fig. 9b, the

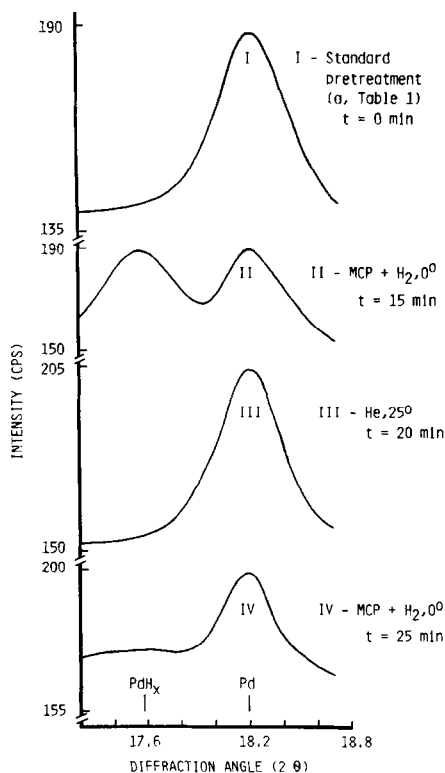


FIG. 6. Diffraction profiles at various stages (I–IV) in Fig. 5, starting with stored catalyst. MCP = methylcyclopropane.

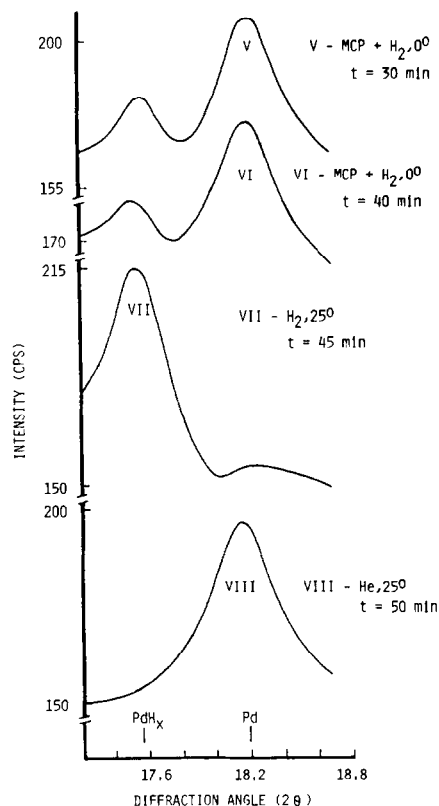


FIG. 7. Diffraction profiles at various stages (V–VIII) in Fig. 5.

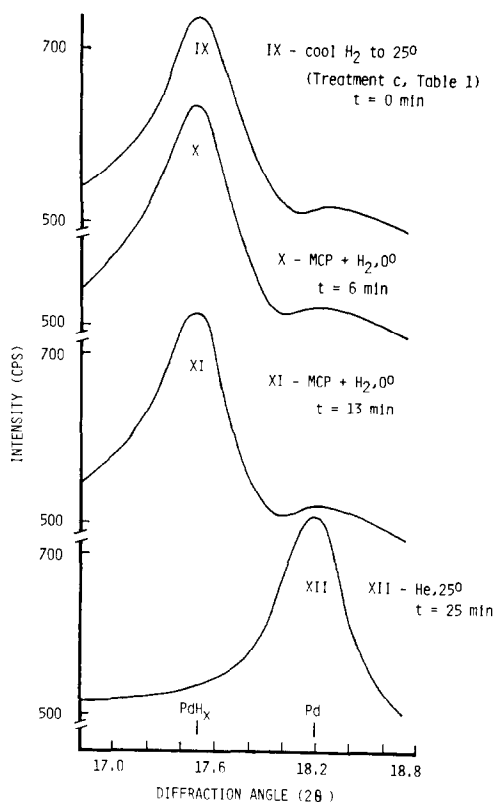


FIG. 8. Diffraction profiles at various stages (IX–XII) in Fig. 5, starting with  $\beta$ -PdH<sub>0.7</sub>.

intensity increased to that characterizing pure Pd over a period of 105 sec. Since about 12 sec was required for helium to reach the catalyst, the actual conversion of the  $\beta$ -hydride in the X-ray beam to Pd

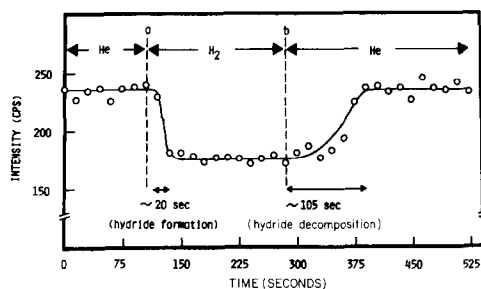


FIG. 9. Intensity in cps vs time for (a) formation and (b) decomposition of hydride at 25°C measured at the 111 peak maximum. Stored Pd/SiO<sub>2</sub> of  $D_h = 13.8\%$  had been exposed to these cycles like those of Fig. 5 before  $t = 0$  min. The points are 15 sec apart (count time was 10 sec and printing time was 5 sec).

occurred in about 90 sec. As is well known (19), the conversion of palladium to  $\beta$ -hydride exhibits hysteresis and formation of hydride occurs only above a  $P_{H_2}$  which is about twice the maximum pressure at which conversion of hydride to Pd can occur. At 25°C, conversion of bulk hydride to Pd occurs only when  $P_{H_2}$  is less than  $\sim 0.01$  atm (19). Since 0.5 cm<sup>3</sup> H<sub>2</sub> is liberated during the conversion of the amount of catalyst employed, a minimum of 50 cm<sup>3</sup> of helium would have to pass through the catalyst bed to remove the 0.5 cm<sup>3</sup> of H<sub>2</sub> at  $P_{H_2} \approx 0.01$  atm. At the flow rate of helium, 3 cm<sup>3</sup>/sec, the minimum time for conversion would be about 16 sec. Pd first appeared in the X-ray beam about 50 sec after switching to helium and complete conversion to Pd then occupied about 50 sec. Thus, conversion of PdH<sub>0.7</sub> to Pd seems to be slower than the reverse reaction. An induction period may be present and the rate of conversion may increase as  $P_{H_2}$  is lowered below 0.01 atm. In this discussion, we have used the value of  $P_{H_2}$  for bulk  $\beta$ -hydride to form Pd. Presumably a larger value would apply to small particles of Pd (see the Introduction) and the calculated minimum time for conversion of the  $\beta$ -hydride to Pd in our catalysts would be smaller than that given above. The alternation between hydrogen and helium was repeated seven times with essentially identical results.

After the standard pretreatment a of the catalyst,  $\beta$ -hydride ( $\sim 50\%$ ) was formed during the reaction (hydrogenolysis at 20% conversion) as shown in Fig. 6. However, if the hydride phase is formed during the pretreatment ( $\sim 90\%$  hydride when cooled from 450°C in hydrogen) as shown in Fig. 8, the composition is not altered by the reaction mixture. The hydride formed in both cases, however, could be removed by a few minute purges of helium either at 25°C or at the reaction temperature. Catalyst with  $D_h = 29.3\%$  showed the same trends but less hydride was formed by treatments b and c (80 vs 90%). It has been suggested in the



past that hydride could be less active than pure Pd because of the filling of the Pd "d" band by the 1s electron of the hydrogen or because of the formation of a new (bulk d) band structure for the hydride.

During hydrogenolysis,  $C_4H_8 + H_2 \rightarrow C_4H_{10}$ , hydrogen adsorbs on the surface of the palladium particles to form  $H^*$  and surface  $H^*$  reacts with adsorbed  $C_4H_8$  to form  $C_4H_{10}$ . The virtual pressure (23) of hydrogen from  $H^*$  must be less than  $P_{H_2}$  in the gas phase if the hydrogenolysis is to occur at a finite rate. At a particular temperature, the value of the virtual pressure during hydrogenolysis will depend upon the rate constant for adsorption of hydrogen, upon that for reaction of adsorbed hydrogen, and upon  $P_{H_2}$  and  $P_{C_4H_8}$ . When we started with catalyst in the Pd form, the ratio PdH/Pd was  $\sim 0.5$  during reaction, although there was some variation in the ratio. From this result it can be concluded that the virtual pressure of  $H^*$  was considerably less than the gas-phase  $P_{H_2}$  and slightly more than the  $P_{H_2}$  required for complete conversion to  $\beta$ -hydride. The residual unhydrided Pd presumably consisted of those particles of Pd which were too small to form  $\beta$ -hydride at the virtual pressure of  $H_2$  at the surface of these particles. Of course, the virtual pressure may be affected by the various kinds of nonuniformity in the palladium particles and by any temperature gradient through the catalyst bed.

When we started with catalyst in the  $\beta$ -hydride form, no hydride was converted to Pd during flow of methylcyclopropane-hydrogen over an interval of 19 min. Apparently, then, there are two steady states depending upon whether the catalyst is initially in the Pd or in the  $\beta$ -hydride form. The higher activity of the catalyst cooled in helium vs that cooled in hydrogen can then, at least in part, be ascribed to a higher content in Pd in the first case. Presumably, the lack of conversion of  $\beta$ -hydride to Pd is associated with the hysteresis observed in the conversion of  $\beta$ -hydride to Pd, that is,

$PdH_{0.7} \rightarrow Pd$  would be fast only when the virtual pressure of hydrogen was substantially below the value at which  $\beta$ -hydride would be formed from Pd.

#### CONCLUSIONS

(1) Techniques for *in situ* examination of catalysts have been demonstrated, both for batch and flow processes.

(2)  $\beta$ -PdH<sub>0.7</sub> forms when a Pd catalyst is cooled from pretreatment in  $H_2$ , exposed to  $H_2$  at room temperature or to a mixture of hydrogen and methylcyclopropane. This supports the proposed explanation for the decrease in activity with such treatments.

(3) The formation exhibits hysteresis; it is easier to form the hydride than to eliminate it. As a result two steady states can exist during hydrogenolysis depending upon whether one starts with catalyst in the Pd or in the PdH form.

(4) The hydride forms throughout a Pd particle, not just at its surface.

(5) The less hydride present the smaller the metal particle size.

(6) The lattice parameter of the Pd particle is the same as that of the bulk, at least down to sizes of  $\sim 45$  Å.

#### ACKNOWLEDGMENTS

This research was supported by the DOE under Grant DE-AC02-77ER04254. The X-ray studies were carried out in the X-ray facility which is supported in part by the NSF-MRL program under Grant NSF-MRL-76-80847 through Northwestern University's Materials Research Center.

#### REFERENCES

1. Graham, T., *Phil. Trans. Roy. Soc. London* **156**, 4151 (1866).
2. Palczewska, W., in "Advances in Catalysis and Related Subjects," Vol. 24, p. 245. Academic Press, New York/London, 1975.
3. Everett, D. H., and Sermon, P. A., *Z. Phys. Chem. N.F.* **114**, 101 (1979).
4. Borodzinski, A., Dus, R., Frak, R., Janko, A., and Palczewska, W., in "Proceedings, 6th International Congress on Catalysis, London, 1976" (G. C. Bond, P. B. Wells, and F. C. Tompkins, Eds.), p. 150. The Chemical Society, London, 1977.
5. Boudart, M., and Hwang, H. S., *J. Catal.* **39**, 44 (1975).

6. Aben, P. C., *J. Catal.* **10**, 224 (1968).
7. Uchijima, T., Herrmann, J. M., Inoue, Y., Burwell, R. L., Jr., Butt, J. B., and Cohen, J. B., *J. Catal.* **50**, 464 (1977).
8. Sashital, S. R., Cohen, J. B., Burwell, R. L., Jr., and Butt, J. B., *J. Catal.* **50**, 479 (1977).
9. Otero-Schipper, P. H., Wachter, W. A., Butt, J. B., Burwell, R. L., Jr., and Cohen, J. B., *J. Catal.* **50**, 494 (1977).
10. Inoue, Y., Herrmann, J. M., Schmidt, H., Burwell, R. L., Jr., Butt, J. B., and Cohen, J. B., *J. Catal.* **53**, 401 (1978).
11. Otero-Schipper, P. H., Wachter, W. A., Butt, J. B., Burwell, R. L., Jr., and Cohen, J. B., *J. Catal.* **53**, 414 (1978).
12. Nandi, R. K., Molinaro, F., Cohen, J. B., Burwell, R. L., Jr., and Butt, J. B., to be submitted.
13. Kobayashi, M., Inoue, Y., Takahashi, N., Burwell, R. L., Jr., Butt, J. B., and Cohen, J. B., *J. Catal.* **64**, 74 (1980).
14. Wong, S. S., Otero-Schipper, P. H., Wachter, W. A., Inoue, Y., Kobayashi, M., Butt, J. B., Burwell, R. L., Jr., and Cohen, J. B., *J. Catal.* **64**, 84 (1980).
15. Pitchai, R., Takahashi, N., Burwell, R. L., Jr., Butt, J. B., and Cohen, J. B., to be submitted.
16. Horvath, B., Mösele, R., Horvath, E. G., and Krauss, H. L., *Z. Anorg. Allg. Chem.* **418**, 1 (1975).
17. Mikkola, D. E., Ph.D. dissertation, Northwestern University, Evanston, Ill., 1964.
18. Macgillavry, C. H., and Rieck, G. D. (Eds.), "International Tables for X-ray Crystallography," Vol. 3, Kynoch Press, Birmingham, England, 1968.
19. Lewis, F. A., "The Palladium Hydrogen System," Academic Press, New York/London, 1967.
20. Flynn, P. C., and Wanke, S. E., *J. Catal.* **34**, 390, 400 (1974).
21. Granqvist, C. G., and Buhrman, R. A., *J. Catal.* **42**, 477 (1976).
22. Wong, S. S., Ph.D. dissertation, Northwestern University, Evanston, Ill., 1980. Available from University Microfilms, Ann Arbor, Mich.
23. Butt, J. B., "Reaction Kinetics and Reactor Design," Prentice-Hall, Englewood Cliffs, N.J., 1980.